PERGAMON

Vision Research 43 (2003) 1091–1102

Vision Research

www.elsevier.com/locate/visres

Position, size and luminosity of phosphenes generated by direct optic nerve stimulation

Jean Delbeke, Medhy Oozeer, Claude Veraart *

Neural Rehabilitation Engineering Laboratory, Université Catholique de Louvain, 54, Avenue Hippocrate, Box UCL 54.46, B-1200 Brussels, Belgium

Received 29 April 2002; received in revised form 9 September 2002

Abstract

Pulses of low intensity current, delivered through a cuff electrode chronically implanted around the optic nerve of a blind retinitis pigmentosa patient generate visual sensations. These phosphenes are obtained at lower thresholds for a train of stimuli than for single pulses, which suggests the existence of a spatial and temporal integrating mechanism. The perceptions are much smaller than those predicted from model simulations. A set of equations are derived which show the effect of pulse current, duration, number and frequency on the position, size and, to some extent, luminosity of the resulting phosphenes.

Keywords: Visual prosthesis; Functional electrical stimulation; Optic nerve; Perceived position; Psychophysics

1. Introduction

Brindley and Lewin made the first attempt to develop a visual prosthesis (Brindley & Lewin, 1968). Since their experiments on direct stimulation of the cortex, three other methods have been developed. These include a stimulation device on the surface of the retina (Humayun et al., 1996), underneath the retina (Zrenner et al., 1997) or a cuff electrode around the optic nerve (Veraart et al., 1998). The last three approaches are based on the observation that in some cases of total blindness and mainly in retinitis pigmentosa, a significant number of ganglion cells and their axons survive and could be usefully activated by such implanted devices (Delbeke et al., 2001; Santos et al., 1997; Stone, Barlow, Humayun, de Juan, & Milam, 1992).

Each of the proposed techniques is expected to artificially generate visual sensations called phosphenes. It is hoped that these can be assembled to produce a useful perception (Zrenner, 2002). The differences between the various methods involve much more than the localisation of the electrode array. The cortical stimuli must take into account complex topological distortions (Brindley, 1970; Normann, Warren, Ammermuller, Fernandez, & Guillory, 2001) and poorly known phosphene psychophysics (Normann, Maynard, Rousche, & Warren, 1999). The sub-retinal devices, on the other hand, could be based on a straightforward pixel organisation (Stett, Barth, Weiss, Haemmerle, & Zrenner, 2000). Both epiretinal and optic nerve stimulation must take the poorly understood retinal encoding into account.

It is also very difficult to predict how the electrode array will perform during stimulation. However, the problem of establishing the exact structures, localisation and size of elements being stimulated can be predicted through modelling of the retina (Greenberg, Velte, Humayun, Scarlatis, & de Juan, 1999; Weiland et al., 1999). Similarly, a dual volume conductor and optic nerve axon model has been developed (Parrini, Delbeke, Legat, & Veraart, 2000; Parrini, Delbeke, Romero, Legat, & Veraart, 1999) that provides topographic maps of the activated zones in the optic nerve stimulated with a spiral cuff electrode (Veraart, Grill, & Mortimer, 1993).

During stimulation of the human optic nerve, phophenes are perceived which are described as clusters of 2–60 dots sometimes arranged in rows or arrays (Veraart et al., 1998). The dot diameter ranged from 8 to 42 min of arc. Occasionally, the phosphenes had a solid appearance. The phosphene encompass an area between 1 and 50 square degrees. Various colours and colour combinations were perceived. It has been possible to

* Corresponding author. Tel.: +32-2-764-5446; fax: +32-2-764-9422.
E-mail address: veraart@gren.ucl.ac.be (C. Veraart).

0042-6989/03/$ - see front matter
doi:10.1016/S0042-6989(03)00013-0

arrange the phosphenes to produce identifiable patterns (Veraart et al., 2001). The optic nerve has now been stimulated about 4 years in a safe and reproducible way (Delbeke et al., 2002). We therefore conclude that a useful optic nerve visual prosthesis is feasible.

Before this is achieved however, a precise correlation between stimulation parameters and the characteristics of the perceived phosphenes must be established (Abbas & Riener, 2001). As a first step, this study will explore the perception threshold as well as the luminosity, size and position of the phosphenes obtained. The relationship between stimulus parameters and these characteristics will be analysed. A comparison was made between the obtained results and a neurophysiological prediction.

2. Material and methods

2.1. The volunteer

This project fully complies with the Declaration of Helsinki, and was approved by the Ethics Committee of the School of Medicine and University Hospital of the Universitéde Louvain, Brussels (Veraart et al., 1998). In addition, special care was take to inform all candidates as completely and exactly as possible (Delbeke et al., 2001). The only volunteer finally implanted is a lady suffering from an autosomal dominant form of retinitis pigmentosa. Her symptoms first appeared when she was 28 years old. She became totally blind (no useful light perception) at age 57 and was implanted with a four-contact cuff electrode (Veraart et al., 1998) 2 years later. At that time, her eye fundi had a classical appearance for retinitis pigmentosa with a pale papilla, narrow blood vessels and pigment deposits. There was a diffuse atrophy of the pigmented epithelium and choriocapillaris except for a small island at the posterior pole. Her optic nerve diameter was 2.7 mm as seen on a pre-surgical MRI scan and then later confirmed during the operation. The transcutaneous leads were replaced with an antenna and telemetry system 30 months after the initially operation. Data obtained in the first 50 days postoperatively have been discarded because of acute changes in the period immediately following electrode implantation. The present study thus relates the remaining 885 days between the two surgical steps.

2.2. Stimulation

Stimuli to the optic nerve were delivered through a 6 mm long self-sizing spiral cuff electrode (Mortimer et al., 1995). The cuff is made of silicon with four recessed (50 μm) pure (99.9%) platinum contacts of 0.2 mm^2, which are located 90° apart around the optic nerve perimeter. Consequently the electrode contacts are referred to as 0°, 90°, 180° and 270°. The electrode was implanted intracranially, just anterior to the chiasm with contact 0° facing the middle lower nasal quadrant, contact 90° the upper nasal, contact 180° the upper temporal and 270° the lower temporal. The position of the contacts was later confirmed by X-ray imaging.

An external stimulator delivered biphasic rectangular current pulse trains of up to 17 pulses at a frequency ranging from 10 to 320 Hz (rarely 1000 Hz was used). The charge-compensating phase of each pulse was at least 5 times longer than the active one, with no delay between them. The cathodic phase had a duration (D) ranging from 21 to 400 μs with amplitudes (I) up to 3.8 mA.

All the results presented below have been obtained with single pulses or short pulse trains which yield instantaneous perceptions, often compared to a flash. No attempt was made to obtain continuous perceptions.

Care was taken never to exceed charge densities of 150 μC/(cm^2 phase) up to 50 Hz and 50 μC/(cm^2 phase) up to 330 Hz. A skin electrode (over the left mastoid) was used as anode.

Current intensity required to reach phosphene perception threshold was defined as I_V. With a pulse intensity I above threshold, the stimulus strength (S) was defined as:

$$S \equiv \left(\frac{I - I_V}{I_V} \right) \times 100\% \quad (1)$$

2.3. Data collection

Phosphene localisation was studied with the volunteer sitting in front of a 45 cm radius hemisphere, her chin and forehead resting on a frame such that her right eye laid in the centre of the hemisphere. The volunteer was asked to fixate at a central reference point on which she held her left index finger as described in (Veraart et al., 1998). After each stimulation and provided the stimulus was above threshold, the volunteer indicated the position of the perception location with her right hand. Meridians and parallels traced on the hemisphere allowed the operator to draw a scheme of the perception on a grid with azimuth (α) and elevation (ε) co-ordinates as described in (Bishop, Kozak, & Vakkur, 1962). Phosphene position and size were documented according to the volunteer's description, as shown with her right index finger on the hemisphere while her left index finger remained on the reference point. The drawings were transferred with 0.35° accuracy (SD) to a numerical database with square pixels of 1° resolution using a graphic tablet. Whenever appropriate for analysis, azimuth or elevation were transformed into eccentricity (w) and position angle (θ) (ω and ψ respectively in Bishop et al., 1962). The position angle is defined as the angle around the visual axis with right horizontal zero.

The phosphene 'area' was defined as the sum of pixels representing the phosphene, neglecting any fine structure. This leads to substantial error with the perceptions limited to a few small separate points. The area equivalent disk radius ρ will be used in the calculations. Phosphene 'position' refers to the average coordinates of its pixels. A luminosity grading scale was defined as follows: 0 = no perception; 0.5 = not sure; 1 = very very (=extremely) dim; 2 = very dim; 3 = dim; 4 = average; 5 = moderately luminous; 6 = luminous; 7 = bright; 8 = very bright; 9 = very very (=extremely) bright. Phosphene perception thresholds were measured using the two-staircase method (Delbeke et al., 2001).

The experimental procedure varied according to the purpose of the test. For threshold measurements, the stimulation current was first set at a value expected to be below threshold and was increased in a stepwise manner. At each step, the perceived phosphenes were recorded as described by the volunteer. When a perception occurred in at least two successive intensity levels, the current was reduced again by the same stepwise method until no perception was elicited. The threshold current was then calculated as the average between the threshold intensities at which the phosphenes first appeared or disappeared as obtained in the ascending and descending series respectively.

In some experiments we investigated the change in phosphene characteristics following small current changes. The protocol consisted of a single increasing series from near threshold level up to the maximal safety limit. No threshold measurement is available for these results.

All the procedures above were repeated for different pulse duration, train length and frequency. For a limited number of trials, each of these parameters was varied while the current was kept constant.

2.4. The '*volume conductor*' model

We attempted to relate the stimulus parameters with the character of the volunteer's perception. Unfortunately there are no means by which to measure the distribution of axons activated during stimulation. For qualitative comparisons, however, this activation map can be estimated from volume conductor modelling (Parrini et al., 1999). This method is divided in two parts. First, the potential fields generated by the stimulation are calculated on a three-dimension finite element geometry (Parrini et al., 1999). Secondly, fibre activation is determined on the basis of the obtained potential field and of a specific set of equations describing optic nerve fibre behaviour (Parrini et al., 2000). This 'volume conductor' model is based on numerous simplifications. We assume that there is a homogeneous distribution of fibres across the nerve and that the optic nerve centre corresponds to the fixation point. The nerve is considered as completely symmetric around the position angle θ. Furthermore, a magnification factor has been applied to the nerve radius. A rough estimation of the required factor has been calculated from available cortical data (Hubel & Wiesel, 1977) and retinal cell counts (Jonas, Schmidt, Muller-Bergh, Schlotzer-Schrehardt, & Naumann, 1992a; Jonas, Schneider, & Naumann, 1992b; Wassle, Grunert, Rohrenbeck, & Boycott, 1990). In both cases, the following transformation can be used as a first approximation:

$$x = 1.685(1 - e^{-w/3.8}) \quad (2)$$

where x is the eccentricity in the optic nerve expressed in mm and w is the corresponding eccentricity in the visual field expressed in degrees.

3. Results

3.1. Perception threshold

Perception threshold is defined as the level of current required for the stimulation to elicit a phosphene perception in two successive steps. Corresponding to the four panels of Fig. 1, the threshold (I_V) has been explored as a function of pulse duration for single pulses and pulse trains. As would be expected from classical excitable membrane physiology (Hill, 1934), the phosphene perception threshold (I_V) is much reduced by lengthening the stimulation pulse duration (Veraart et al., 1998).

Interestingly, Hill's equation can be fitted to the thresholds obtained by single pulse (Fig. 1A) as well as train stimulation (Fig. 1B) with the same time constant (c) of 188 μs. The rheobase (I_r) i.e. the threshold obtained from very long duration pulses, differ greatly (−0.21 mA for single pulses in A and −0.052 mA for the 9 pulse trains at 80 Hz in B). The rheobase has been further explored as a function of the number (N) of pulses and their frequency (F). As shown in Fig. 1C and D, a marked reduction of the perception threshold was observed when either frequency or number of pulses increased. In terms of Hill's strength–duration equation, this means that the rheobase value for phosphene perception generated by pulse train stimuli varies with the pulse number and frequency, leading to the following expression:

$$I_V = \frac{I_r(N,F)}{1 - e^{-D/c}} \quad (3)$$

where D is the individual pulse duration.

The threshold changes are most important for pulse intervals greater than 10 ms (below 100 Hz in Fig. 1C).

If a long train (e.g. $N = 30$) has pulse duration and amplitude values just above perception threshold, then a

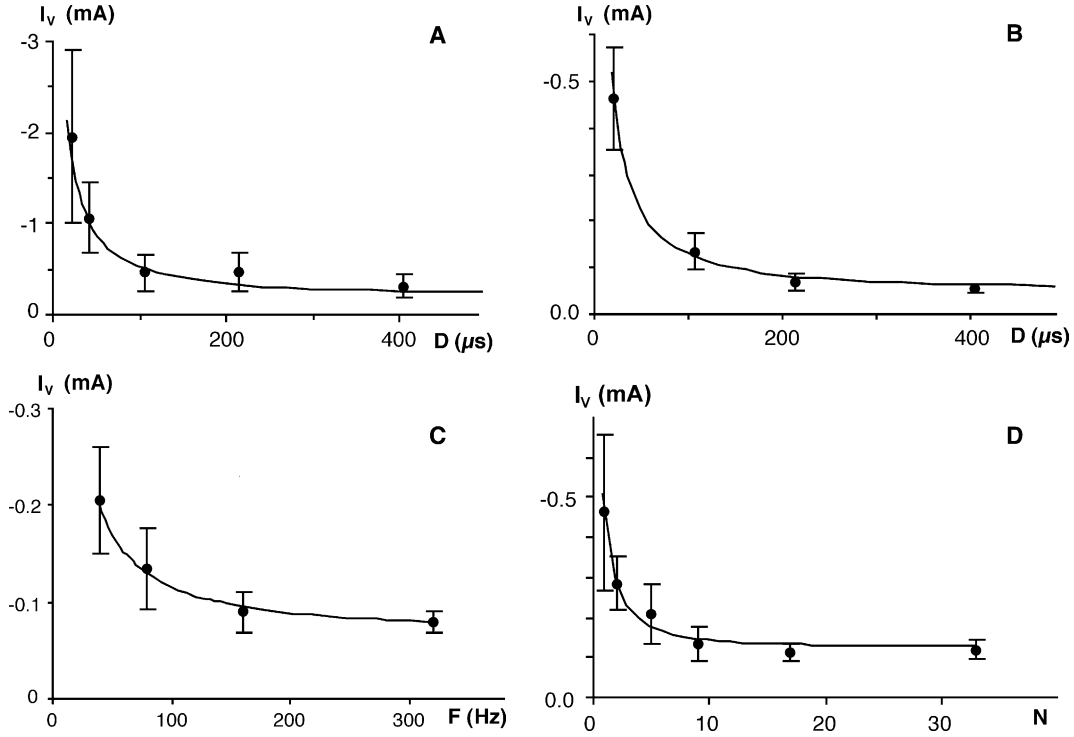

Fig. 1. Visual perception threshold currents as a function of the stimulation pulse duration, frequency and number. Dots represent average thresholds. Standard deviations are given as error bars. The continuous traces correspond to the threshold model results. (A) 70 measurements with single pulse stimulation; (B) 25 measurements with 9 pulse trains at 80 Hz. Eq. (3) with a common time constant of 188 μs has been fitted in A and B. Note the different ordinate scales and hence rheobases; (C) 38 measurements for trains of 9 pulses (duration 106.5 μs); (D) 92 measurements for trains at 80 Hz (pulse duration 106.5 μs). The model traces in C and D correspond to Eq. (4) with the same time constant as in A and B.

shorter train (of say $N = 3$) of identical pulses will no longer reach perception threshold (see Fig. 1D). In both cases, the same axons are activated by each single pulse. This suggests that perception results from a temporal summation of the effect of each pulse in a train. Next, with the same subthreshold train (i.e. $N = 3$), increasing the stimulus intensity will result in the recruitment of more fibres in the nerve and a spatial summation will lead to perception again. A mechanism has thus been hypothesised whereby perception thresholds can be reached either through spatial summation (each single pulse recruit more axons), or by temporal summation (repeated activation of a few axons) in the case of train stimulation (Delbeke, Parrini, Glineur, Vanlierde, & Veraart, 1999).

Straightforward accumulation of electric charge at the level of the axonal membrane is not possible with biphasic pulses. The ionic membrane mechanisms involved in the axonal relative refractory and supernormal periods (Adrian & Lucas, 1912) could hardly play a role. Indeed, according to personal simulations and animal experimental results (George, Mastronarde, & Dubin, 1984), at pulse frequencies (about 100 Hz) where these effects seem to be maximal, they first lead to a threshold increase and only to a threshold decrease of a mere 10% with long stimulation trains. In fibres subthresholdly stimulated, this effect will be much smaller if at all present. Stimulating repeatedly with the same pulse can thus hardly be expected to result in more fibres to be recruited, at least not in the time domain and at the scale shown in Fig. 1C and D. By the all-or-none principle, with short duration pulses as used here, increasing the stimulus amplitude is not expected to change the response of already active axons, but new ones will be recruited. Phenomena such as a possible anodal block have been considered but studies show that they would require much higher current levels than used in this study. A central integration mechanism has therefore been hypothesised which has been formalised in the following perception threshold model:

$$I_V = \frac{g\sum_{i=1}^{N} e^{(i-N)/(\tau F)} + P_S(h-2g)}{(1-e^{-D/c})\left(\sum_{i=1}^{N} e^{(i-N)/(\tau F)} - P_S\right)} \quad (4)$$

Details about the origin of this equation can be found in the Appendix A. In brief, it is identical to Eq. (3) with the rheobase term I_r expanded in a temporal summation term (function of the pulse number (N) and frequency (F)) and three parameters added which represent the spatial recruitment of fibres in the optic nerve. These last are: g is the rheobase current for activation of the first optic nerve axon recruited, h is the current level at which the rheobase level has been reached for half the axon

population, P_S is the proportion of axons activated at perception threshold by a single isolated pulse, τ is time constant of an EPSP-like contribution of each axonal firing to the alleged summation.

The various parameters have been estimated by fitting the threshold model to the 215 threshold measurements available, yielding $c = 188$ μs, $\tau = 0.071$ s; $g = 14.9$ μA; $h = 2181$ μA; $P_S = 0.083$ as average values for the four contacts. The perception threshold model results have been plotted as a line over each of the panels of Fig. 1, showing a close correlation to the experimental data.

More formally, a determination coefficient r^2 of $0.81[t(213) = 30; p < 0.001]$ is obtained between the experimental thresholds and the perception threshold model results. The distribution of the threshold deviation from the expected values is roughly Gaussian with a standard deviation of 36%.

Below is a description of the correlation between phosphene characteristics and stimulation parameters, including pulse intensity, duration, number and frequency. The expected thresholds are calculated as just described. A major advantage of using S (see Eq. (1)) is that the effect of pulse number, frequency, duration and current can be pooled together. For all the experimental sessions where no threshold measurement was available, the value was replaced in the calculation of S by the estimation of Eq. (4).

3.2. Phosphene luminosity

Despite the fact that the subjective luminosity scale was defined from 0 to 9, most (98.9%) of the levels reported by the volunteer ranged from 0 to 4 ('average'). The few brighter perceptions were so rare that they might correspond to technical artefacts and have therefore been rejected. The remaining 1413 recordings have been represented in a grey scale histogram as a function of the stimulus strength (S) and the perceived luminosity (Fig. 2A). Average values are also plotted as individual points. These have been fitted with the curve:

$$L = 2.76 + 0.066\sqrt{S} \tag{5}$$

Luminosity is not very dependent on the stimulus parameters ($r^2 = 0.18$ for S, leaving no more than 1% residual variance explained by D, N or F). The luminosity tends to be weaker but much more variable near threshold. In many cases, the perceived luminosity near threshold is as good as at high stimulation strengths. It is typically described by the volunteer as 'average'. No significant difference was found between the results obtained from stimulation via each of the four contacts. The reported luminosity levels are stable in the sense that they do not correlate with time since implantation.

3.3. Phosphene size

Phosphenes are described as solid patches of light, groups of points or lines in a single restricted area of the visual field. In the following we refer only to the area occupied by the phosphene and ignore its texture. Phosphene size is the sum of the pixels necessary to draw the perceived phosphene. For a given stimulation condition, the size is variable and distribution histograms have been made for three subgroups of tests characterised by different stimulation strengths: $S \leqslant 30\%$, $30 < S < 200\%$, $S \geqslant 200\%$. The corresponding average diameters are 2.96°, 4.51°, 6.15° respectively with the following variances: 2.10°, 4.45°, 7.18°. Fig. 2B shows the distribution as a function of ρ, the equivalent disk radius. If R is the average value of ρ in each group, then, these distributions closely match the Poisson equation

$$\Pr(2\rho) = \frac{(2R)^{2\rho}}{(2\rho)!}\mathrm{e}^{-2R} \tag{6}$$

with R respectively equal to 1.61°, 2.23° and 3.46°.

A determination coefficient $r^2 = 0.34[t(663) = 18.6; p < 0.001]$ is obtained with the following regression between equivalent radius and stimulation strength.

$$\rho = 1.63 + 0.012S \tag{7}$$

D, N or F would each account for less than 5% of the remaining variability of ρ as estimated from r^2.

3.4. Phosphene position

All phosphenes obtained in this study were restricted to an area of the visual field between −30° and +30° horizontally and from +20° to −50° vertically. At first sight, the localisation of the phosphene centres seems rather random. There is a clear trend (Fig. 3) however for the phosphenes generated by the 270° contact to be located in the upper left field, while the lower left is reached by the 180° contact and the lower right by the 90° contact. Only phosphenes generated by the 0° can be found in the upper right field. The upper visual field is much less well covered than the lower field. In Fig. 3, results have been separated on the basis of the stimulation train characteristics. Single pulses and short or low frequency trains have been represented in the left panel while the right panel displays responses to long and high frequency trains. These later stimulus characteristics obviously extend the part of the visual field that can be reached. The wide range of these train parameters in our experimental conditions contributes to the dispersion of the position for low stimulation strength (open triangles). In all cases high strength levels (open circles) yield more central positions. Again, inclusion of results obtained at different strength levels do increase the variance especially at intermediary levels. A more precise correlation will be shown hereafter.

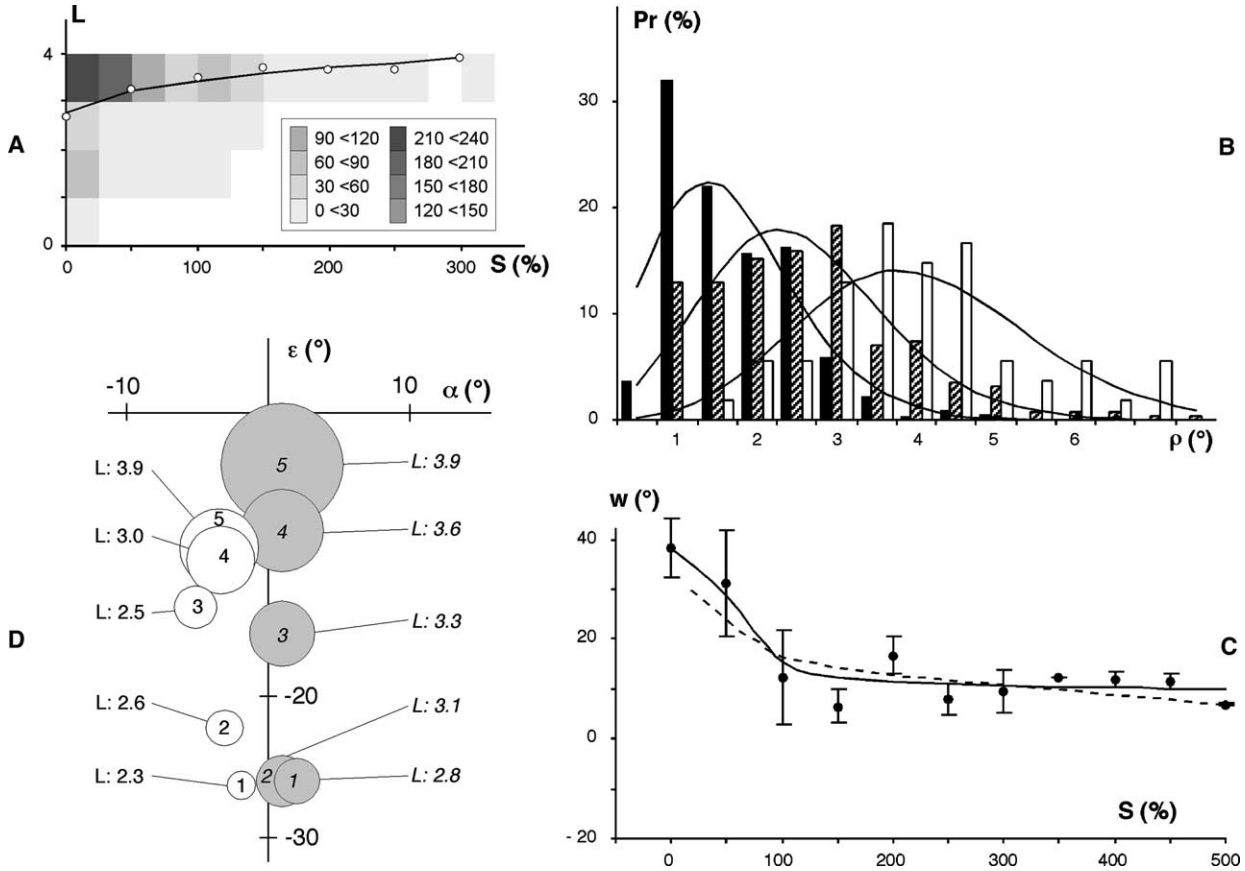

Fig. 2. Phosphenes luminosity, position and size. (A) Perceived luminosity (L) versus stimulus strength (S) for all 1411 phosphenes. Each grey rectangle represents the number of phosphene records as defined in the inset. Open dots stand for average luminosity values that have been fitted with a solid line described by Eq. (5). (B) Phosphene area. Bars represent the probability (in %) to find a phosphene whose equivalent disk radius (ρ) is given in abscissa. Black bars for $S < 30\%$; hatched bars for $30\% \leqslant S < 200\%$; white bars for $S \geqslant 200\%$. The superimposed traces show Poisson (Eq. (6)) distributions fitted to the equivalent diameter distributions. (C) Mean (dashed line) and standard deviation (error bars) of phosphene eccentricity (w) versus S for 71 stimulation tests at contact 90° fitted with a solid line described by Eq. (9). Dashed line: position of the midpoint of the activation field margin for axons of 0.6 μm diameter as simulated with the volume conductor model. (D) Comparison between experimental data and the phosphene model predictions for migration with stimulus strength. Position, size and luminosity (L labels) are provided for both the phosphene model predictions (grey disks) and experimental results (white disks) for different S values as indicated within each disk (1: 0%; 2: 25%; 3: 75%; 4: 150%; 5: 300%). In both cases, the stimulation conditions were contact 180°, trains of 9 pulses of 42.6 μs at 160 Hz.

The average phosphene eccentric position near threshold is labelled A. As we have seen in Fig. 3, when S is increased, the eccentricity reduces and phosphenes location ultimately stabilises at a central position B (Fig. 2C). Point B is reached when S is greater than 200%. This migration phenomenon is similar to the stimulus intensity dependent shift of the midpoint of the margin of the activation maps, as predicted from the volume conductor model. This is drawn as a dotted line in Fig. 2C.

An average of the co-ordinates of 54 experimental values obtained at $S \geqslant 200\%$ is given in Table 1 as the position of point B. As could be expected from the summation effects on the threshold intensity described above, the position of point A is variable and depends on the stimulus parameters. Except for contact 270°, where migration is hardly seen, the best predictor for A appears to be the ratio P_S/P_N (see Appendix A, Eq. (A.7)) with the following linear regression:

$$A = v + u \sum_{i=1}^{N} e^{(i-N)/(\tau F)} \tag{8}$$

Eq. (8) applies to w and θ co-ordinates, the corresponding values of v and u being estimated from 355 experimental data obtained at $S < 30\%$.

In analogy with phosphene migration (Appendix A, Eq. (A.2)) and the shift of the recruitment curve margin (Fig. 2C and Fig. 4A1–C1), the following function was derived:

$$Z = A + (B - A)\left(\frac{S - s}{S + m - 2s}\right) \quad \text{with } Z = A \text{ if } S < s \tag{9}$$

where Z represents either w or θ depending on which set of constants is used. Characteristic constants s and m represent the S values at onset of migration and at the

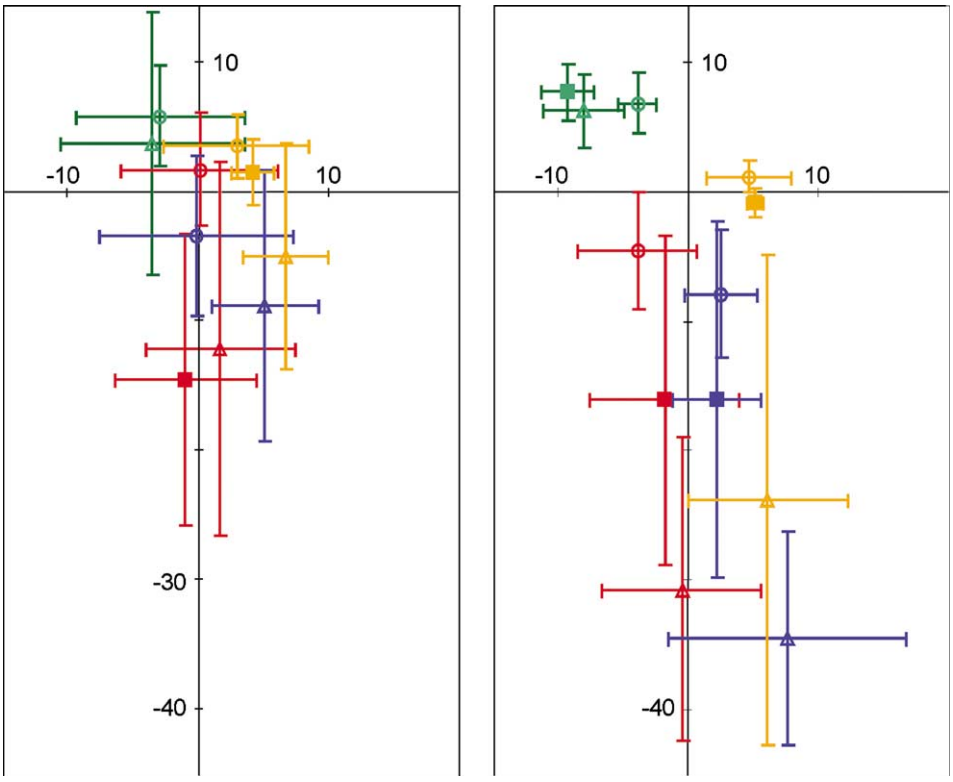

Fig. 3. Phosphene centre positions as recorded. Average position and SD are displayed in azimuth (α = ordinate) and elevation (ε = abscissa) co-ordinates. Colours refer to the contact giving rise to the corresponding phosphenes: 0° = yellow; 90° = blue; 180° = red; 270° = green. Open triangles represent near-threshold results up to a strength of 30. The filled squares display the data for $30 > S > 200$ and the open circles stand for $S \geqslant 200$. Only recordings for whose a threshold measurement (used to calculate S) was obtained during the same session are included. Results obtained with single pulses, short or low frequency trains ($P_S/P_N < 6$ according to Eq. (A.7) in Appendix A) are represented on the left panel (number of experimental data = 81, 88, 110 and 69 for contacts 0°, 90°, 180° and 270° respectively). The right panel holds the remaining results for $P_S/P_N > 6$ with (number of experimental data = 40, 126, 102 and 49 for contacts 0°, 90°, 180° and 270° respectively).

point where the phosphene is located half way between A and B respectively. Eq. (9) was fitted to the 256 results of migration experiments with S values between 30 and 200. Table 1 provides the constants of Eqs. (8) and (9) as related to each contact.

Globally, the model yields an r^2 value of $0.54[t(663) = 27.7; p < 0.001]$ and $0.50[t(663) = 25.5; p < 0.001]$ for w and θ respectively.

The phosphene model Eqs. (5)–(9) were briefly assessed during five additional sessions. The results are illustrated in Fig. 2D where a set of experimental results (white disks) representing phosphene position and size are plotted next to the corresponding modelled phosphenes (shaded).

3.5. Fibre recruitment

Phosphenes migrate according to changes in stimulus parameters as described above. They remain relatively small-sized even when large stimulating currents are used which activate a large number of fibres in the optic nerve. It is not possible to directly measure the activity within the optic nerve during stimulation. However, the

Table 1
Parameters for the eccentricity (w) and inclination (θ) model of Eqs. (8) and (9) as estimated by fitting these equations to the experimental data

Contact	u_w (°)	u_θ (°)	v_w (°)	v_θ (°)	B_w (°)	B_θ (°)	s_w (%)	s_θ (%)	m_w (%)	m_θ (%)
0°[a]	2.40	−3.55	6.37	−36.35	2.73	13.98	5.07	0	14.82	56.14
90°[b]	3.68	−3.13	5.80	−54.74	9.06	−84.06	40.22	0	54.00	0.69
180°[b]	3.05	−3.43	7.81	−67.48	1.15	−145.10	32.47	−1	107.61	0
270°[c]	−0.33	−6.23	12.32	−153.40	5.75	−224.96	0	85.72	999,999	123.13

[a] Significant correlation between model and data ($p < 0.001$) for w and θ.
[b] Significant correlation between model and data ($p < 0.001$) for w only.
[c] Significant correlation between model and data ($p < 0.001$) for θ only.

volume conductor model can offer a qualitative basis to estimate the activation map.

As is shown by the coloured crescents in Fig. 4A–C, increasing the stimulus current (0.10, 0.15 and 0.20 mA respectively, in the example) from threshold to higher values results in ever more axons being activated. Each colour corresponds to a different fibre diameter. Because the activation maps overlap, only the edges are shown but the activation starts near the stimulating contact for all diameters. The activation maps expand towards the nerve centre when the stimulus intensity is increased. A projection of the activation maps in the visual field is shown in the corresponding Fig. 4A1–C1. Due to the magnification factor (Eq. (2)), limit of the activated region moves even faster towards the centre. The model simplifications and approximations can not account for this qualitative observation.

Phosphenes as large as the projection of the activated region, and occupying about half the visual field, have never been reported by the volunteer. On the contrary, the little white disks as shown in Fig. 4 (right column) have been drawn to represent actual phosphenes as observed in similar stimulation conditions. They are very small and move towards the visual field centre as the stimulation strength increases, as described above.

4. Discussion

4.1. A single case study

The scope of this study is limited to just a single case. This is mainly due to ethical reasons. We do not consider implanting any more volunteers until the prosthesis has been thoroughly investigated and has been shown to be potentially useful. However, our observations must, in due course, be confirmed in other volunteers to establish any inter-subject variability.

4.2. Effects of the disease

Retinitis pigmentosa represents the final target group for the visual prosthesis. Our results are obtained from a patient with a very severe form of the disease and therefore cannot be extrapolated to the physiology of healthy humans. Physiological interpretations should take into account that at least 20–40% of axons could be lost through secondary trans-synaptic degeneration of the ganglion cells (Humayun et al., 1999). This comes in addition to the known axonal loss with ageing (Balazsi, Rootman, Drance, Schulzer, & Douglas, 1984; Jonas et al., 1992a, 1992b). Based on the regression given by Jonas et al. (Jonas, Schmidt, Muller-Bergh, & Naumann, 1995), we find that our volunteer would have around 630,000 axons in her optic nerve. There is no reason to believe that the remaining functional axons are homogeneously distributed. Retinotopically or functionally specific subpopulations could have been differently affected. A predominant loss of retinal ganglion cells in the peripheral field has been shown to exist in retinitis pigmentosa (Humayun et al., 1999). This could explain why we were unable to generate phosphenes in the most lateral and upper visual fields. Phosphenes generated with the 0° and 270° contacts do not show the extensive migration observed with the 90° and 180° contacts, perhaps simply because there is no substrate available for them to appear in the periphery of the corresponding sector. Years of blindness could also result in visual field calibration errors (Li & Matin, 1992). This would in turn result in distortions of the phosphene localisation in our study.

4.3. The perception time issue

According to our results, a stimulus of say 4 pulses delivered at high frequency and of such duration and current amplitude that the perception threshold is just reached, would be expected to be peripherally located. If the stimulation does not stop there and that 20 more pulses of the same amplitude and duration are delivered, the resulting stimulation train would have a 'strength' far above threshold. The resulting phosphene would thus expectedly be located in the central visual field. In other words, when a long train resulting in a central phosphene is being delivered it first reaches a stage where it is identical to a short train known to yield a peripheral perception. Long stimulation trains can thus be expected to generate 'multiple' or 'moving' or 'stretched' such that they include a peripheral perception as well as a more central one. This is never the case in our observations. The perception of the longer stimulus does not include awareness of an intermediary stage. It seems that conscious perception only takes place at the end of the temporal summation. This is in keeping with the known fact that the conscious perception time is not synchronous to the arrival of afferent signals to the brain while the subjective timing can still correspond to the stimulus onset (Libet, Wright, Feinstein, & Pearl, 1979). It may be that it is the disruption in the firing rate occurring at the end of the train the provides the trigger leading to the conscious perception of the stimulus as a whole.

4.4. Size and position of the phosphenes

If retinotopy in the optic nerve is considered as a point-to-point spatial relationship between the nerve section and the retina, then, all that can be said is that stimulation through each of the four contacts tends to result in a phosphene located in the corresponding quadrant of the visual field. Such a rough correspondence was found in earlier tests (Veraart et al., 1998) and

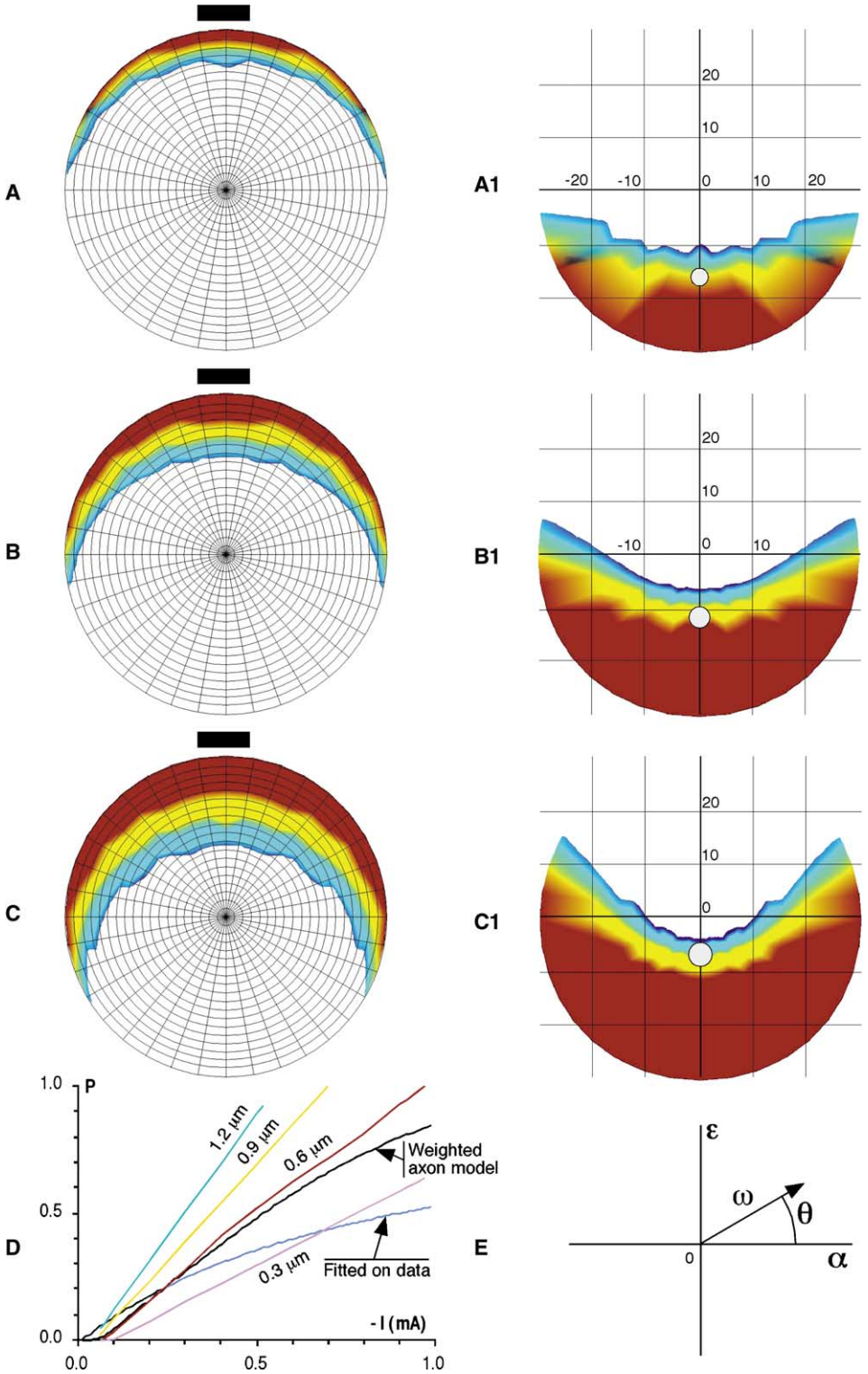

Fig. 4. Activation maps and spatial recruitment. Left column: black bar indicates the stimulation contact position. All colours included in D, refer to a given optic nerve axon diameter: magenta: 0.3 μm, red–brown: 0.6 μm, yellow: 0.9 μm and blue–green: 1.2 μm. A, B and C correspond to stimulation pulses of 0.1, 0.15 and 0.2 mA respectively (pulse duration: 100 μs). (D) Proportion (P) of fibres activated at a given stimulation current intensity. The straight lines correspond to the modelled recruitment of fibres of a single diameter (Eq. (A.1)). The red–brown trace (0.6 μm axon) has been fully drawn from the volume conductor model while the other three are extrapolated from a few points. The black curve is a weighted average of the individual recruitment curves modelling the global recruitment of fibres of all diameters in the optic nerve. The blue curve corresponds to the recruitment function (Eq. (A.2)) with the parameters providing the best fit of Eq. (4) with the experimental threshold data. Right column: A1 to C1 are the projections of the activated fibres onto the visual field limited to the central 60°. These projections take a central magnification factor into account. White disks superimposed on these maps represent average phosphene as observed for a train stimuli of 5 pulses for 100 μs duration, at the same current intensity as in A, B and C respectively and delivered at 100 Hz through contact 180°. (E) Co-ordinates used in this study.

is confirmed here. Any encoding of spatial information in the optic nerve distorts the relationship between position of a given axon in the optic nerve and corresponding sensations in the visual field. The models described here show that this complex relationship can at least be partially described. Of course, the model predictions are blurred, perhaps due to imperfections in the anatomical retinotopy as observed in animal experiments (Fitzgibbon & Taylor, 1996; Naito, 1989) but also due to psycho-physical inaccuracies. Our results suggest that phosphenes typically appear near the margin of the region of projection of the optic nerve fibres activation map. This characteristic is also true for the 0° contact although in this case, the radial direction along which this phenomenon appears is rather unexpected.

A large proportion of activated fibres seem not to contribute topologically to phosphene perception. It is unlikely that conduction block and similar mechanisms are at play in our results because of the very low stimulation currents used especially with train stimuli. One possibility could be that in those regions, equal amounts of activated ON and OFF fibres cancel each other out at a central level, which would not be the case at the margin of the activated region. However, collateral inhibition as it exists in the lateral geniculate nucleus (Sherman & Koch, 1986) could perhaps generate the same edge-limited perception. Still, the relationship between activation maps in the optic nerve and the position, size and shape of the phosphenes is complex and cannot be explained in terms of our present knowledge.

4.5. Phosphene luminosity

Except very near threshold, the perceived phosphene luminosity appears to be almost totally independent of the stimulus parameters investigated here. This is in keeping with the finding (Rossi & Paradiso, 1999) that responses in ganglion cells do not correlate with a visual stimulus brightness while this information is present in the cortex. Brightness representation in the optic nerve must thus be part of a relatively complex encoding scheme.

4.6. The variability of the experimental results

We observe some variability in threshold measurements. This could have a large number of potential sources. It is clear that even with direct experiments, responses to luminal stimuli are probabilistic in nature (Carley & Raymond, 1983). Continuous changes in axon threshold are a well-known phenomenon in human electrophysiology (McComas, 1995).

Although the optic nerve seems to be mechanically well protected within the skull, plethysmographic activity and tissue conductivity changes with blood flow pulses could easily affect the stimulation currents. We have indeed observed some oscillations of the thresholds obtained in the second half of the ECG cycle (unpublished observation). Threshold changes due to deleterious effects of the stimulation itself are unlikely because no corresponding trend in threshold was observed.

Moreover, the volunteer occasionally describes spontaneous phosphenes. Such activity might interfere with the artificially elicited perceptions (Usrey, Reppas, & Reid, 1998). Variability could also be of central origin and the activity of neurones is known to be modulated by external factors (Aiello & Bach-Y-Rita, 1997). The response to our stimulation is nothing more than a verbal report by our volunteer about a very weak perception. More global factors such as attention and fatigue should thus be considered as well.

5. Conclusion

Phosphene luminosity, size and position are best predicted on the basis of stimulus intensity in reference to the perception threshold value. The threshold itself is related to the stimulus pulse duration, number and frequency. These relationships can be explained on the basis of the axon membrane strength–duration, the spatial recruitment of fibres across the optic nerve and some synaptic-like temporal summation mechanism.

Equations resulting from these considerations were presented which summarises our results and provide a framework for further explorations. They also represent a necessary tool when the right stimulus parameters have to be chosen in order to generate a phosphene of selected attributes.

From the results presented here, we have learned that the phosphene size is much smaller than expected from the calculation of the activation maps. This small size combined with the possibility to control the localisation of the resulting perception is in favour of a further development of the optic nerve visual prosthesis.

Acknowledgements

Supported by grants from: CEU 'Esprit' #22 527 (MiViP) and IST-2000-25145 (Optivip); FMSR #3.4584.98 and #3.4590.02; the Walloon Region of Belgium #114645; a private donation. We wish to thank our volunteer for her commitment and infinite patience, B. Gérard, G. Michaux and Dr. M.-Ch. Wanet for their help as well as Dr. M. Brelén for reviewing the English language.

Appendix A

Activation maps such as Fig. 4A–C obtained from the volume conductor model, can be used to draw a re-

cruitment curve (percentage of axons activated or probability for any axon to be activated) for an axon of chosen diameter. Based on the volume conductor model (full trace for 0.6 μm axons and linear interpolations for 0.3, 0.9 and 1.2 μm axons in Fig. 4D) the following estimate is obtained for the proportion $P(d)$ of fibres of diameter d (in μm) stimulated by a 100 μs pulse of current I (in mA).

$$P(d) = I(1.6d + 0.142) - 0.066 \tag{A.1}$$

The global proportion of fibres activated by a given current intensity is the weighted average (see Fig. 4D) of Eq. (A.1) for all axon diameters, taking into account the size distribution available in the literature (Jonas, Muller-Bergh, Schlotzer, & Naumann, 1990). At perception rheobase, the proportion P_N of fibres activated by each of the N pulses of a stimulus train will follow the same recruitment curve empirically represented by equation:

$$P_N = \frac{I_r - g}{I_r + h - 2g} \quad \text{for } I_r \geqslant g \tag{A.2}$$

By rearranging Eq. (A.2) and substituting in Eq. (3),

$$I_V = \frac{g + P_N(h - 2g)}{(1 - e^{-D/c})(1 - P_N)} \tag{A.3}$$

If n is the total number of fibres potentially involved in phosphene perception, P_1 the proportion of axons activated at perception threshold by a single pulse, M_N the post-synaptic membrane potential of an hypothetical integrating neurone after stimulation with a train of N pulses, and a the average amplitude contribution of each axonal firing, then, at perception threshold,

$$M_1 = nP_1a + M_0 + M_c$$

where M_0 represents the residual potential generated by previous activity and M_c, the influence of interfering factors such as other synchronous stimuli delivered or background activity. Defining P_S as the value of P_1 when M_0 and M_c are negligible (i.e. in the absence of such interfering activity), then the membrane potential is given by

$$M_S = nP_Sa \tag{A.4}$$

Let the contribution of each axon firing be represented by a simple decreasing exponential with time constant τ and an initial instantaneous amplitude a as a rough analogy to synaptic EPSPs. Then, at perception threshold after a second pulse in a train of frequency F,

$$M_2 = nP_2a(e^{-1/(\tau F)} + 1) + M_0e^{-1/(\tau F)} + M_c$$

By recurrence, the membrane potential for perception threshold at the onset of the last pulse of a train of N pulses at frequency F can be written as

$$M_N = nP_Na\left(\sum_{i=1}^{N} e^{(i-N)/(\tau F)}\right) + M_0e^{-((N-1)/(\tau F))} + M_c \tag{A.5}$$

Considering that at perception threshold, $M_N = M_S$, then the combination of Eqs. (A.4) and (A.5) yields

$$P_N = \frac{P_S - (1/(na))\left(M_c + M_0e^{-((N-1)/(\tau F))}\right)}{\sum_{i=1}^{N} e^{(i-N)/(\tau F)}} \tag{A.6}$$

For isolated train studies, $M_0 = 0$ and $M_c = 0$. Then

$$\frac{P_S}{P_N} = \sum_{i=1}^{N} e^{(i-N)/(\tau F)} \tag{A.7}$$

Eq. (A.7) can be substituted in Eq. (A.3) to obtain the expected perception threshold as given in Eq. (4).

References

Abbas, J. J., & Riener, R. (2001). Using mathematical models and advanced control systems techniques to enhance neuroprosthesis function. *Neuromodulation, 4*, 187–195.

Adrian, E. D., & Lucas, K. (1912). On the summation of propagated disturbance in nerve and muscle. *Journal of Physiology (London)*, 68–124.

Aiello, G. L., & Bach-Y-Rita, P. (1997). Brain cell microenvironment effects on neuron excitability and basal metabolism. *Neuroreport, 8*, 1165–1168.

Balazsi, A. G., Rootman, J., Drance, S. M., Schulzer, M., & Douglas, G. R. (1984). The effect of age on the nerve fiber population of the human optic nerve. *American Journal of Ophthalmology, 97*, 760–766.

Bishop, P. O., Kozak, W., & Vakkur, G. J. (1962). Some quantitative aspects of the cat's eye: axis and plane of reference, visual field coordinates and optics. *Journal of Physiology (London), 163*, 466–502.

Brindley, G. S. (1970). Sensations produced by electrical stimulation of the occipital poles of the cerebral hemispheres, and their use in constructing visual prostheses. *Annals of the Royal College of Surgeons of England, 47*, 106–108.

Brindley, G. S., & Lewin, W. S. (1968). The sensations produced by electrical stimulation of the visual cortex. *Journal of Physiology (London), 196*, 479–493.

Carley, L. R., & Raymond, S. A. (1983). Threshold measurement: applications to excitable membranes of nerve and muscle. *Journal of Neuroscience Methods, 9*, 309–333.

Delbeke, J., Parrini, S., Glineur, O., Vanlierde, A., & Veraart, C. (1999). Phosphene perception thresholds to direct stimulation of a human optic nerve shows spatial and temporal summation. *Society for Neuroscience Abstracts, 25*, 1043 (Abstract).

Delbeke, J., Pins, D., Michaux, G., Wanet-Defalque, M. C., Parrini, S., & Veraart, C. (2001). Electrical stimulation of anterior visual pathways in retinitis pigmentosa. *Investigative Ophthalmology and Vision Science, 42*, 291–297.

Delbeke, J., Wanet-Defalque, M. C., Gerard, B., Troosters, M., Michaux, G., & Veraart, C. (2002). The microsystems based visual prosthesis for optic nerve stimulation. *Artificial Organs, 26*, 232–234.

Fitzgibbon, T., & Taylor, S. F. (1996). Retinotopy of the human retinal nerve fibre layer and optic nerve head. *The Journal of comparative neurology, 375*, 238–251.

George, S. A., Mastronarde, D. N., & Dubin, M. W. (1984). Prior activity influences the velocity of impulses in frog and cat optic nerve fibers. *Brain Research, 304*, 121–126.

Greenberg, R. J., Velte, T. J., Humayun, M. S., Scarlatis, G. N., & de Juan, E., Jr. (1999). A computational model of electrical stimulation of the retinal ganglion cell. *IEEE Transactions on Biomedical Engineering, 46*, 505–514.

Hill, A. V. (1934). The intensity–duration relation for nerve excitation. *Journal of Physiology (London), 83*, 30P (Abstract).

Hubel, D. H., & Wiesel, T. N. (1977). Ferrier lecture. Functional architecture of macaque monkey visual cortex. *Proceedings of the Royal Society of London Series B Biological sciences, 198*, 1–59.

Humayun, M. S., de Juan, E., Jr., Dagnelie, G., Greenberg, R. J., Propst, R. H., & Phillips, D. H. (1996). Visual perception elicited by electrical stimulation of retina in blind humans. *Archives of Ophthalmology, 114*, 40–46.

Humayun, M. S., Prince, M., de Juan, E., Jr., Barron, Y., Moskowitz, M., Klock, I. B., & Milam, A. H. (1999). Morphometric analysis of the extramacular retina from postmortem eyes with retinitis pigmentosa. *Investigative Ophthalmology and Vision Science, 40*, 143–148.

Jonas, J. B., Muller-Bergh, J. A., Schlotzer, S., & Naumann, G. O. (1990). Histomorphometry of the human optic nerve. *Investigative Ophthalmology and Vision Science, 31*, 736–744.

Jonas, J. B., Schmidt, A. M., Muller-Bergh, J. A., & Naumann, G. O. (1995). Optic nerve fiber count and diameter of the retrobulbar optic nerve in normal and glaucomatous eyes. *Graefes Archive for Clinical and Experimental Ophthalmology, 233*, 421–424.

Jonas, J. B., Schmidt, A. M., Muller-Bergh, J. A., Schlotzer-Schrehardt, U. M., & Naumann, G. O. (1992a). Human optic nerve fiber count and optic disc size. *Investigative Ophthalmology and Vision Science, 33*, 2012–2018.

Jonas, J. B., Schneider, U., & Naumann, G. O. (1992b). Count and density of human retinal photoreceptors. *Graefes Archive for Clinical and Experimental Ophthalmology, 230*, 505–510.

Li, W., & Matin, L. (1992). Visual direction is corrected by a hybrid extraretinal eye position signal. *Annals of the New York academy of sciences, 656*, 865–867.

Libet, B., Wright, E. W., Jr., Feinstein, B., & Pearl, D. K. (1979). Subjective referral of the timing for a conscious sensory experience: a functional role for the somatosensory specific projection system in man. *Brain, 102*, 193–224.

McComas, A. J. (1995). Motor-unit estimation: the beginning. *Journal of Clinical Neurophysiology, 12*, 560–564.

Mortimer, J. T., Agnew, W. F., Horch, K., Citron, P., Creasey, G., & Kantor, C. (1995). Perspectives on new electrode technology for stimulating peripheral nerves with implantable motor prostheses. *IEEE Transactions on Neural Systems and Rehabilitation Engineering, 3*, 145–153.

Naito, J. (1989). Retinogeniculate projection fibers in the monkey optic nerve: a demonstration of the fiber pathways by retrograde axonal transport of WGA-HRP. *The Journal of comparative neurology, 284*, 174–186.

Normann, R. A., Maynard, E. M., Rousche, P. J., & Warren, D. J. (1999). A neural interface for a cortical vision prosthesis. *Vision Research, 39*, 2577–2587.

Normann, R. A., Warren, D. J., Ammermuller, J., Fernandez, E., & Guillory, S. (2001). High-resolution spatio-temporal mapping of visual pathways using multi-electrode arrays. *Vision Research, 41*, 1261–1275.

Parrini, S., Delbeke, J., Legat, V., & Veraart, C. (2000). Modelling analysis of human optic nerve fibre excitation based on experimental data. *Medical and Biological Engineering and Computing, 38*, 454–464.

Parrini, S., Delbeke, J., Romero, E., Legat, V., & Veraart, C. (1999). Hybrid finite elements and spectral method for computation of the electric potential generated by a nerve cuff electrode. *Medical and Biological Engineering and Computing, 37*, 733–736.

Rossi, A. F., & Paradiso, M. A. (1999). Neural correlates of perceived brightness in the retina, lateral geniculate nucleus, and striate cortex. *Journal of Neuroscience, 19*, 6145–6156.

Santos, A., Humayun, M. S., de Juan, E., Jr., Greenburg, R. J., Marsh, M. J., Klock, I. B., & Milam, A. H. (1997). Preservation of the inner retina in retinitis pigmentosa. A morphometric analysis. *Archives of Ophthalmology, 115*, 511–515.

Sherman, S. M., & Koch, C. (1986). The control of retinogeniculate transmission in the mammalian lateral geniculate nucleus. *Experimental Brain Research, 63*, 1–20.

Stett, A., Barth, W., Weiss, S., Haemmerle, H., & Zrenner, E. (2000). Electrical multisite stimulation of the isolated chicken retina. *Vision Research, 40*, 1785–1795.

Stone, J. L., Barlow, W. E., Humayun, M. S., de Juan, E., Jr., & Milam, A. H. (1992). Morphometric analysis of macular photoreceptors and ganglion cells in retinas with retinitis pigmentosa. *Archives of Ophthalmology, 110*, 1634–1639.

Usrey, W. M., Reppas, J. B., & Reid, R. C. (1998). Paired-spike interactions and synaptic efficacy of retinal inputs to the thalamus. *Nature, 395*, 384–387.

Veraart, C., Grill, W. M., & Mortimer, J. T. (1993). Selective control of muscle activation with a multipolar nerve cuff electrode. *IEEE Transactions on Biomedical Engineering, 40*, 640–653.

Veraart, C., Raftopoulos, C., Mortimer, J. T., Delbeke, J., Pins, D., Michaux, G., Vanlierde, A., Parrini, S., & Wanet-Defalque, M. C. (1998). Visual sensations produced by optic nerve stimulation using an implanted self-sizing spiral cuff electrode. *Brain Research, 813*, 181–186.

Veraart, C., Wanet-Defalque, M. C., Delbeke, J., Gérard, B., Troosters, M., & Michaux, G. (2001). Assessment of the «MIVIP» optic nerve visual prosthesis. *Investigative Ophthalmology and Vision Science, 42*, S942 (Abstract).

Wassle, H., Grunert, U., Rohrenbeck, J., & Boycott, B. B. (1990). Retinal ganglion cell density and cortical magnification factor in the primate. *Vision Research, 30*, 1897–1911.

Weiland, J. D., Humayun, M. S., Dagnelie, G., de Juan, E., Jr., Greenberg, R. J., & Iliff, N. T. (1999). Understanding the origin of visual percepts elicited by electrical stimulation of the human retina. *Graefes Archive for Clinical and Experimental Ophthalmology, 237*, 1007–1013.

Zrenner, E. (2002). Will retinal implants restore vision? *Science, 295*, 1022–1025.

Zrenner, E., Miliczek, K. D., Gabel, V. P., Graf, H. G., Guenther, E., Haemmerle, H., Hoefflinger, B., Kohler, K., Nisch, W., Schubert, M., Stett, A., & Weiss, S. (1997). The development of subretinal microphotodiodes for replacement of degenerated photoreceptors. *Ophthalmic Research, 29*, 269–280.